



SCUOLA INTERNAZIONALE SUPERIORE DI STUDI AVANZATI

SISSA Digital Library

Exciton condensation in strongly correlated quantum spin Hall insulators

*Original*

Exciton condensation in strongly correlated quantum spin Hall insulators / Amaricci, A.; Mazza, G.; Capone, M.; Fabrizio, M.. - In: PHYSICAL REVIEW. B. - ISSN 2469-9950. - 107:11(2023), pp. 1-8. [10.1103/PhysRevB.107.115117]

*Availability:*

This version is available at: 20.500.11767/133574 since: 2023-08-07T09:29:31Z

*Publisher:*

*Published*

DOI:10.1103/PhysRevB.107.115117

*Terms of use:*

Testo definito dall'ateneo relativo alle clausole di concessione d'uso

*Publisher copyright*

APS - American Physical Society

This version is available for education and non-commercial purposes.

note finali coverpage

(Article begins on next page)

# Exciton condensation in strongly correlated quantum spin Hall insulators

A. Amaricci,<sup>1</sup> G. Mazza,<sup>2,3</sup> M. Capone,<sup>4,1</sup> and M. Fabrizio<sup>4</sup>

<sup>1</sup>*CNR-IOM, Istituto Officina dei Materiali, Consiglio Nazionale delle Ricerche, Via Bonomea 265, 34136 Trieste, Italy*

<sup>2</sup>*Dipartimento di Fisica, Università di Pisa, Largo Bruno Pontecorvo 3, 56127, Pisa, Italy*

<sup>3</sup>*Department of Quantum Matter Physics, University of Geneva,*

*Quai Ernest-Ansermet 24, 1211 Geneva, Switzerland*

<sup>4</sup>*Scuola Internazionale Superiore di Studi Avanzati (SISSA), Via Bonomea 265, 34136 Trieste, Italy*

Time reversal symmetric topological insulators are generically robust with respect to weak local interaction, unless symmetry breaking transitions take place. Using dynamical mean-field theory we solve an interacting model of quantum spin Hall insulators and show the existence, at intermediate coupling, of a symmetry breaking transition to a non-topological insulator characterised by exciton condensation. This transition is of first order. For a larger interaction strength the insulator evolves into a Mott one. The transition is continuous if magnetic order is prevented, and notably, for any finite Hund's exchange it progresses through a Mott localization before the condensate coherence is lost. We show that the correlated excitonic state corresponds to a magneto-electric insulator which allows for direct experimental probing. Finally, we discuss the fate of the helical edge modes across the excitonic transition.

The concept of symmetry protected topology has introduced a new paradigm for the description of electronic band structures [1, 2]. The early identification of topological states in semi-conducting quantum wells [3, 4] and three-dimensional chalcogenides [5–8] boosted intense research activity that finally reached a mature symmetry groups classification for weakly-interacting insulators and semi-metals. The discovery of topological properties in more correlated materials [9, 10], such as monolayers of early transition-metals dichalcogenides (TMD)s [11–13] or some Fe-based compounds [14–18], raised interest in the role of the ever-present electron-electron interaction in topological phases of matter.

The electron localization tendency brought in by strong correlations can generically lead to dramatic modifications of the band structure topology [19]. Contrary to naïve expectations, Coulomb repulsion can in some cases favour the formation of a non-trivial electronic state [10, 20], trigger the existence of novel purely interacting topological phases [21], or drive a dynamical change in the thermodynamic character of the topological quantum phase transition [22–25]. Yet, the most impactful effect of strong electronic correlations is often the emergence of ordered phases. At strong coupling, the existence of large spin-exchanges and spin-orbit coupling paves the way to magnetically ordered states. For weaker interaction strength, the situation can get more intriguing since diverse degrees of freedom are equally active and possibly cooperate with the non-trivial topology of the electronic bands. In these conditions, different instabilities compete and it becomes hard to predict the electronic properties of a correlated topological insulator.

One of the most interesting effect of electronic interaction in systems hosting a small energy gap is to induce in-gap excitons [26–31]. Although excitons have been studied for long, recent evidences supporting the existence of excitonic phases in TMDs mono-layers [11–13, 32] gave strong impulse to the investigation of excitons in topological insulators [26, 28, 30]. For instance, the anomalies

observed in the topological Kondo insulator  $SmB_6$  have been predicted to be caused just by excitons [33–37].

Here, we show that exciton phase transition generically occurs due to electronic correlations in a model quantum spin Hall insulator (QSHI). In particular, using a non-perturbative approach based on Dynamical Mean-Field Theory (DMFT) [38–40], we demonstrate that, in presence of a sufficiently strong interaction, the QSHI becomes unstable towards an excitonic phase with an in-plane spin polarisation [28, 41] that breaks the time-reversal, spin  $U(1)$  and parity symmetries [30] that protect topological order. The transition between the QSHI and the Excitonic Insulator (EI) is of first order within DMFT. The excitonic phase shows a finite magneto-electric susceptibility [42, 43], which allows a direct experimental identification of such state of matter.

The rest of the paper is organized as follows. In the Sec. I we introduce the interacting QSHI model and briefly recall the method used to solve it. In the following section II we discuss the excitonic phase transitions occurring for generic values of the parameters, distinguishing the two cases corresponding to the presence or the absence of Hund's exchange. We summarize part of the findings in terms of phase-diagram in Sec. III. In the section IV we discuss observable consequences of the excitonic transition in the QSHI. Finally, in Sec. V we draw the conclusions of our work and discuss some perspectives.

## I. MODEL AND METHODS

We consider an interacting two-orbital Hubbard model on a two dimensional square lattice [3, 22], described by the Hamiltonian

$$H = \sum_{\mathbf{k}} \psi_{\mathbf{k}}^{\dagger} H(\mathbf{k}) \psi_{\mathbf{k}} + H_{int}, \quad (1)$$

with the spinor  $\psi_{\mathbf{k}}^{\dagger} = [c_{\mathbf{k}1\uparrow}^{\dagger}, c_{\mathbf{k}2\uparrow}^{\dagger}, c_{\mathbf{k}1\downarrow}^{\dagger}, c_{\mathbf{k}2\downarrow}^{\dagger}]$  and where  $c_{\mathbf{k}\alpha\sigma}^{\dagger}$  creates an electron on orbital  $\alpha = 1, 2$ , with spin  $\sigma = \uparrow, \downarrow$  at momentum  $\mathbf{k}$ . Orbital 1 and 2 transform as the  $\ell = 0$  and  $\ell = 1$  spherical harmonics, respectively [3], and, more specifically,

$$\begin{aligned} (2, \uparrow) &\equiv (\ell = 1, \ell_z = +1, \uparrow), \\ (2, \downarrow) &\equiv (\ell = 1, \ell_z = -1, \downarrow), \end{aligned}$$

are the  $j_z = \pm 3/2$  components of  $j = 3/2$  spin-orbit multiplet.

We introduce the  $4 \times 4$  matrix basis  $\Gamma_{\alpha a} = \sigma_{\alpha} \otimes \tau_a$ , where  $\sigma_{\alpha=0,1,2,3}$  and  $\tau_{a=0,1,2,3}$  are Pauli matrices, including the identity, in spin and orbital subspaces, respectively. The non-interacting Hamiltonian matrix reads

$$H(\mathbf{k}) = M(\mathbf{k}) \Gamma_{03} + \lambda \sin(k_x) \Gamma_{31} - \lambda \sin(k_y) \Gamma_{02}, \quad (2)$$

where  $M(\mathbf{k}) = M - \epsilon(\cos k_x + \cos k_y)$ ,  $M \geq 0$  being the energy separation between the two orbitals,  $\epsilon$  the hopping amplitude and  $\lambda$  the inter-orbital hybridization that lacks an on-site component because of inversion symmetry. Hereafter, we take  $\epsilon = 1$  as our unit of energy,  $\lambda = 0.3$ , and assume two electrons per site, i.e. half-filling. The non-interacting Hamiltonian is invariant under Time Reversal Symmetry  $\mathcal{T}$  (TRS), inversion symmetry  $\mathcal{P}$ ,  $U(1)$  spin rotations around the  $z$ -axis, and the fourfold  $C_4$  spatial rotations around  $z$ . We assume that the interaction is also invariant under the same symmetries, and, in particular, we take

$$H_{int} = \frac{1}{4} \sum_{\mathbf{r}} (2U - 3J) \hat{N}_{\mathbf{r}}^2 - J \hat{S}_{z\mathbf{r}}^2 + 2J \hat{T}_{z\mathbf{r}}^2, \quad (3)$$

where  $\mathbf{r}$  labels the sites of the lattice, and the operators

$$\begin{aligned} \hat{N}_{\mathbf{r}} &= \psi_{\mathbf{r}}^{\dagger} \Gamma_{00} \psi_{\mathbf{r}}, \\ \hat{S}_{z\mathbf{r}} &= \frac{1}{2} \psi_{\mathbf{r}}^{\dagger} \Gamma_{30} \psi_{\mathbf{r}}, \\ \hat{T}_{z\mathbf{r}} &= \frac{1}{2} \psi_{\mathbf{r}}^{\dagger} \Gamma_{03} \psi_{\mathbf{r}}, \end{aligned}$$

with  $\psi_{\mathbf{r}}$  the Fourier transform of  $\psi_{\mathbf{k}}$ , are, respectively, the density, the spin polarization along  $z$  and the orbital polarization at site  $\mathbf{r}$ . The interaction (3) is not the most general symmetry allowed one. However, it enforces the first Hund's rule of maximum spin, whose role we aim to analyse here.

We treat the interaction non-perturbatively by single-site DMFT using exact diagonalization as impurity solver [44]. Within DMFT, the self-energy is approximated by a momentum independent but frequency dependent matrix function in spin and orbital space. A symmetry invariant self-energy matrix is diagonal, with spin-independent elements. Deviations from such matrix structure signal the onset of symmetry breaking [24, 28, 41, 45–49]. The non-interacting model has a topological quantum phase transition between a QSHI for  $M < 2$  and a trivial Band Insulator (BI) for  $M > 2$ . In the presence of a finite Hund's

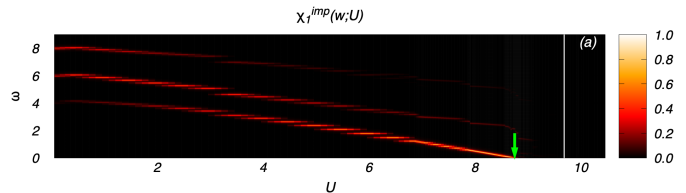


Figure 1. Evolution of the low-energy spectra of the in-plane triplet component of the exciton-exciton susceptibility  $\chi_1^{imp}(\omega)$  as a function of the interaction strength  $U$ . Data for  $J/U = 0.25$  and  $M = 3.5$ . The arrow indicate the softening of the lowest energy peak before Mott insulator sets in (white solid line).

exchange  $J$  and for large  $U$ , see Eq. (3), a high-spin Mott insulator sets in [22, 48, 50] and describes two electrons localized on each site and forming a spin  $S_z = \pm 1$  configuration, thus with vanishing orbital polarization  $T_z = 0$ .

## II. THE EXCITONIC PHASE-TRANSITION

In order to assess the possible instability of the model towards an excitonic phase it is instructive to start from the atomic limit with two electrons per site. The Hamiltonian in the two-electron subspace reads

$$H_{at} = \sum_{\mathbf{r}} -J \hat{S}_{z\mathbf{r}}^2 + 2J \hat{T}_{z\mathbf{r}}^2 + 2M \hat{T}_{z\mathbf{r}}.$$

The eigenstates can be labelled by the eigenvalues  $S_z, T_z$  and  $\ell_z$ , respectively, of the operators  $\hat{S}_{z\mathbf{r}}, \hat{T}_{z\mathbf{r}}$  and

$$\hat{\ell}_z = n_{2\uparrow\mathbf{r}} - n_{2\downarrow\mathbf{r}},$$

with  $n_{\alpha\sigma\mathbf{r}} = c_{\alpha\sigma\mathbf{r}}^{\dagger} c_{\alpha\sigma\mathbf{r}}$ . Thus the states  $|(\ell_z, S_z, T_z), \mathbf{r}\rangle$  have eigenvalues  $E(\ell_z, S_z, T_z)$ :

$$\begin{aligned} E(0, 0, +1) &= 2J + 2M, \\ E(0, 0, -1) &= 2J - 2M, \\ E(+1, +1, 0) &= E(-1, -1, 0) = -J, \\ E(+1, 0, 0) &= E(-1, 0, 0) = 0. \end{aligned} \quad (4)$$

For  $3J > 2M$  the atomic ground state is the high-spin doublet with  $S_z = \pm 1$ , otherwise is the state  $|(0, 0, -1), \mathbf{r}\rangle$  with two electrons in orbital 2. Our aim is to study the competition between those states, and therefore we hereafter drop the other three states,  $|(0, 0, +1), \mathbf{r}\rangle$  and  $|(\pm 1, 0, 0), \mathbf{r}\rangle$ .

Moreover, we define a pseudo spin operator  $\mathbf{I}_{\mathbf{r}} = (I_{x\mathbf{r}}, I_{y\mathbf{r}}, I_{z\mathbf{r}})$  through

$$\begin{aligned} I_{z,\mathbf{r}}|(+1, +1, 0), \mathbf{r}\rangle &\equiv I_z|+1, \mathbf{r}\rangle = |+1, \mathbf{r}\rangle, \\ I_{z,\mathbf{r}}|(0, 0, -1), \mathbf{r}\rangle &\equiv I_z|0, \mathbf{r}\rangle = 0, \\ I_{z,\mathbf{r}}|(-1, -1, 0), \mathbf{r}\rangle &\equiv I_z|-1, \mathbf{r}\rangle = -|-1, \mathbf{r}\rangle, \end{aligned}$$

so that the three states become the components of an  $I = 1$  pseudo spin. In this subspace the following equivalences

hold

$$\begin{aligned}\psi_{\mathbf{r}}^\dagger \Gamma_{11} \psi_{\mathbf{r}} &\equiv \sqrt{2} I_{x\mathbf{r}}, & \psi_{\mathbf{r}}^\dagger \Gamma_{21} \psi_{\mathbf{r}} &\equiv \sqrt{2} I_{y\mathbf{r}}, \\ \psi_{\mathbf{r}}^\dagger \Gamma_{12} \psi_{\mathbf{r}} &\equiv -\sqrt{2} \{I_{y\mathbf{r}}, I_{z\mathbf{r}}\}, & \psi_{\mathbf{r}}^\dagger \Gamma_{22} \psi_{\mathbf{r}} &\equiv -\sqrt{2} \{I_{x\mathbf{r}}, I_{z\mathbf{r}}\}, \\ \psi_{\mathbf{r}}^\dagger \Gamma_{03} \psi_{\mathbf{r}} &\equiv 2(1 - I_{z\mathbf{r}}^2), & \psi_{\mathbf{r}}^\dagger \Gamma_{30} \psi_{\mathbf{r}} &\equiv 2I_{z\mathbf{r}},\end{aligned}$$

while  $\psi_{\mathbf{r}}^\dagger \Gamma_{\alpha a} \psi_{\mathbf{r}}$  with all other  $\Gamma$  matrices different from the identity have vanishing matrix elements.

The atomic Hamiltonian projected onto the subspace  $|0, \mathbf{r}\rangle$  and  $|\pm 1, \mathbf{r}\rangle$  becomes, dropping constants:

$$H_{\text{at}} \simeq \Delta E \sum_{\mathbf{r}} \left(1 - I_{z\mathbf{r}}^2\right), \quad \Delta E = 3J - 2M.$$

Our interest is studying how the hopping processes beyond the atomic limit modify the level crossing between  $|\pm 1, \mathbf{r}\rangle$  and  $|0, \mathbf{r}\rangle$  when  $\Delta E$  changes sign. For that, we treat those processes at second order in perturbation theory and, after projection onto the above subspace, we find an effective Heisenberg Hamiltonian for the  $I = 1$  pseudo spins

$$\begin{aligned}H_* &= \Delta E_* \sum_{\mathbf{r}} \left(1 - I_{z\mathbf{r}}^2\right) \\ &+ J_+ \sum_{\langle \mathbf{r}\mathbf{r}' \rangle} \left(2 I_{z\mathbf{r}} I_{z\mathbf{r}'} - \sum_{a=x,y} I_{a\mathbf{r}} I_{a\mathbf{r}'}\right) \\ &+ J_- \sum_{\langle \mathbf{r}\mathbf{r}' \rangle} \left(K_{z\mathbf{r}} K_{z\mathbf{r}'} - \sum_{a=x,y} K_{a\mathbf{r}} K_{a\mathbf{r}'}\right),\end{aligned}\quad (5)$$

where  $K_{a\mathbf{r}} = \{I_{a\mathbf{r}}, I_{z\mathbf{r}}\}$ , while

$$\Delta E_* = \Delta E + 8J_-, \quad J_{\pm} = \frac{1 \pm \lambda^2}{4U}.$$

When  $\Delta E_* \gg J_+ > J_-$ , the ground state is a Néel antiferromagnet with  $\langle I_{z\mathbf{r}} \rangle = (-1)^{\mathbf{r}}$ . On the contrary, when  $\Delta E_* \ll -|J_+|$ , each site in the ground state is locked into the  $I_z = 0$  eigenstate of the pseudo-spin triplet, which is just the trivial band insulator since the topological one does not survive in the atomic limit. These two states might cross in energy when  $\Delta E_* \simeq 0$ , but that crossing is preempted by the quantum fluctuations brought about by  $J_+$  and  $J_-$  that, in turn, compete against each other. Since  $J_+$  is larger, we can safely neglect  $J_-$ . In that case, the Hamiltonian (5) describes an easy-axis spin-1 Heisenberg antiferromagnet with a single-ion anisotropy  $\Delta E_*$ , which suggests that the transition between the Néel antiferromagnet and the band insulator might occur through an intermediate phase characterised by the order parameter

$$\begin{aligned}\Delta(\phi) &= \langle I_{x\mathbf{r}} + I_{y\mathbf{r}} \rangle = \frac{1}{\sqrt{2}} \langle \psi_{\mathbf{r}}^\dagger (\Gamma_{11} + \Gamma_{21}) \psi_{\mathbf{r}} \rangle \\ &\equiv \Delta_{11} + \Delta_{21} = \Delta \cos(\phi) + \Delta \sin(\phi)\end{aligned}\quad (6)$$

which breaks  $\mathcal{T}$ , inversion symmetry  $\mathcal{P}$  and spin  $U(1)$  symmetry for any fixed value of  $\phi \in [0, 2\pi)$  [30]. This

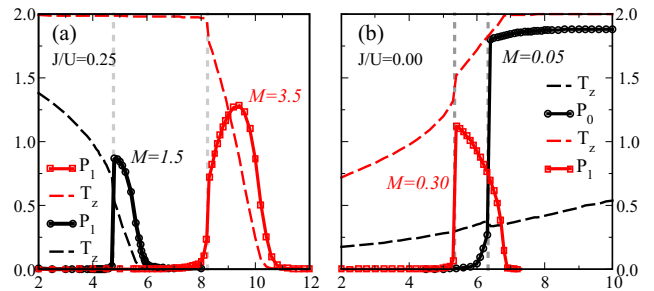


Figure 2. Orbital polarization  $T_z$  (dashed lines) and exciton order parameter  $P_1$  (solid line and symbols) as a function of the interaction strength  $U$  at  $J = 0.25U$ , left panel, and  $J = 0$ . For the  $J = 0$  case, we also show the order parameter  $P_0$  corresponding to the formation of an odd-parity spin-singlet excitonic state, which is always zero at  $J = 0.25U$ .

phase actually describes a condensate of odd-parity spin-triplet excitons, with the spin lying in the  $x - y$  plane.

To assess whether such excitonic phase indeed exists and does survive at intermediate coupling, we have calculated the dynamical susceptibility  $\chi_{11}^{imp}(\omega) = \frac{1}{N} \int dt e^{i\omega t} \langle T_t [\mathbb{F}_{11}(t) \mathbb{F}_{11}(0)] \rangle$  forcing all symmetries within the effective impurity problem of the DMFT [38] and where  $\mathbb{F}_{\alpha a} = \psi^\dagger \Gamma_{\alpha a} \psi$  [28, 30] are impurity operators. Although this quantity does not necessarily correspond to the local susceptibility of the bulk model, nonetheless it provides suitable informations about its instabilities. In Fig. 2(a) we report the evolution of  $\chi_{11}^{imp}(\omega)$ , which is equivalent to  $\chi_{21}^{imp}(\omega)$  by spin  $U(1)$  symmetry, as a function of energy  $\omega$  and  $U$  at  $M = 3.5$ , thus along the path from the band to the Mott insulator. In the weakly interacting regime, this function displays several high energy peaks. Increasing  $U$  leads to red shift of the lowest energy peak until it softens before the Mott transition sets in. The softening is just the signal of the excitonic instability.

However, the conclusive proof of excitonic transition can be obtained allowing for symmetry breaking, which we do though forcing, for simplicity, translational symmetry. Our results are reported in Fig. 2 for  $J = 0.25U$ , left panel, and  $J = 0$ , right panel.

### A. The $J > 0$ case

For any  $M > 0$  we observe the formation of an EI with

$$P_1 = \langle \psi_{\mathbf{r}}^\dagger \Gamma_{11} \psi_{\mathbf{r}} \rangle \neq 0,$$

which is related to  $\langle \psi_{\mathbf{r}}^\dagger \Gamma_{21} \psi_{\mathbf{r}} \rangle$  under spin  $U(1)$ , see Eq. (6). The transition from the band or topological insulators to the excitonic one is of first order, while that from the EI to the high-spin Mott insulator (hs-MI) is of second order. We cannot exclude that also the latter transition may become first order allowing for transla-

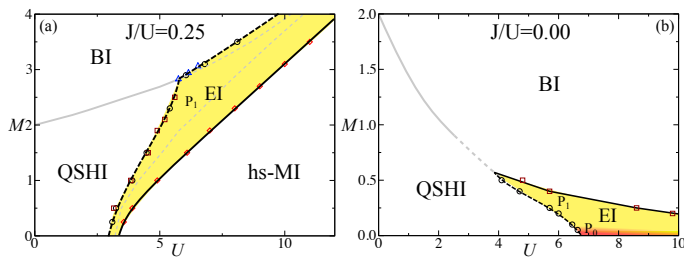


Figure 3. DMFT phase diagrams of the interacting model as a function of  $U$  and  $M$ . Left panel (a) for  $J/U = 0.25$ . Right panel (b) for  $J = 0$ . The nature of the leading excitonic order parameter is indicated in the plot using text and color code. First order transition are indicated with dashed lines. Continuous transitions are indicated with solid lines. Transitions to/from EI are indicated in black. Gray lines in the background indicate the transitions occurring without allowing for exciton condensation.

tional symmetry breaking, and thus for an antiferromagnetic Mott insulator [24].

The order parameter  $P_1$  as a function of  $U$  displays a bell-like structure, which is centred at increasing values of  $U$  as  $M$  grows. Interestingly, the peak value is attained at different positions depending on the nature of the uncorrelated insulator. For  $M < 2$  (QSHI) the peak value is reached immediately after the transition while for  $M > 2$  (BI) the peak is well inside the excitonic region. We also observe that the orbital polarisation  $T_z$  vanishes before the Mott transition, i.e., when  $P_1$  is still finite.

### B. The $J = 0$ case

At  $J = 0$ , the atomic levels (4) include the ground state  $|0, 0, -1\rangle$ , followed at energy  $2M$  above by the fourfold multiplet  $|\pm 1, \pm 1, 0\rangle$  and  $|\pm 1, 0, 0\rangle$ , and, finally, by  $|0, 0, +1\rangle$  at energy  $4M$  above the ground state. For large  $U$ , the hopping at second order in perturbation theory generates superexchange processes of order  $1/U$ . Therefore, the model at  $U \rightarrow \infty$  and finite  $M$  describes just the band insulator with two electrons in orbital 2. However, the situation may change if  $M$  scales as  $1/U$ . In that case, and if we discard the highest energy atomic level  $|0, 0, +1\rangle$ , the superexchange processes mix the atomic ground state  $|0, 0, -1\rangle$  with the first excited multiplet on nearest neighbour sites. Similarly to the  $J > 0$  case, these processes may lead to finite expectation values of the local operators that have finite matrix elements between  $|0, 0, -1\rangle$  and the fourfold multiplet  $|\pm 1, \pm 1, 0\rangle \oplus |\pm 1, 0, 0\rangle$ . We already showed that at  $\lambda \neq 0$  the mixing between  $|0, 0, -1\rangle$  and the doublet  $|+1, +1, 0\rangle \oplus |-1, -1, 0\rangle$  stabilises the order parameters  $P_1 = \langle \psi_{\mathbf{r}}^\dagger \Gamma_{11} \psi_{\mathbf{r}} \rangle$  and its spin- $U(1)$  partner  $\langle \psi_{\mathbf{r}}^\dagger \Gamma_{21} \psi_{\mathbf{r}} \rangle$ . Similarly, the order parameters  $P_0 = \langle \psi_{\mathbf{r}}^\dagger \Gamma_{01} \psi_{\mathbf{r}} \rangle$  and its  $C_4$  partner  $\langle \psi_{\mathbf{r}}^\dagger \Gamma_{32} \psi_{\mathbf{r}} \rangle$ , which thus break  $C_4$  and inversion symmetries, are favoured by the mixing between  $|0, 0, -1\rangle$  and the doublet  $|+1, 0, 0\rangle \oplus |-1, 0, 0\rangle$  at  $\lambda \neq 0$ .

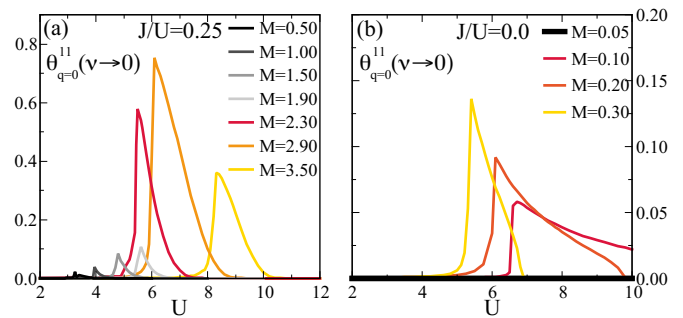


Figure 4. Static and uniform limit of the magnetic-electric susceptibility as a function of the interaction strength  $U$  across the exciton phase transition. Data are for different values of  $M$ , as indicated in the panels, and for (a)  $J/U = 0.25$ , (b)  $J/U = 0.00$ .

Our explicit DMFT calculations predict that, at  $M \sim 1/U$ ,  $P_1$  is always stabilised except at very small  $M$ , where the order parameter  $P_0$  prevails, see right panel of Fig. 2. We further observe that at  $J = 0$  the transition from the QSHI to the EI is still first order, while that from the EI to the BI is continuous.

### C. Phase diagrams

We summarize our DMFT results in the two  $U$  vs.  $M$  phase diagrams at  $J > 0$  and  $J = 0$ , respectively, left and right panels in Fig. 3. In both cases, the non-interacting QSHI-BI transition point at  $M = 2$  transforms at weak-coupling into a critical line determined by the condition

$$M_{\text{eff}} \equiv M + \frac{1}{4} \text{Tr} (\Gamma_{03} \Sigma(\omega = 0)) = 2,$$

where  $\Sigma(\omega)$  is the self-energy matrix. The critical line corresponds to a second order phase transition up to a critical value of the interaction  $U_c$ . For  $U > U_c$ , the transition turns first order [22, 23, 51], thus without crossing a Dirac-like gapless point.

For  $J > 0$  and large enough  $U$ , the ground state describes a high-spin Mott insulator. An extended EI region with  $P_1$  order parameter intrudes between the QSHI and the hs-MI, see Fig. 3(a). Remarkably, the EI phase entirely covers the discontinuous topological transition occurring between the BI and the QSHI. The transitions from either the BI or the QSHI to the EI are of first order, while the transition from the EI to the hs-MI is continuous.

At  $J = 0$ , we observe an EI region between the QSHI and the BI at small  $M < 0.5$ . The QSHI-to-EI and EI-to-BI transitions are, respectively, of first and second orders. For very large  $U$ , the EI phase appears at  $M$  scaling as  $1/U$ . As we mentioned, the exciton condensate with order parameter  $P_0$ , breaking  $C_4$  and inversion symmetries, for very small  $M$ , while for larger values, the order parameter  $P_1$  prevails, breaking inversion, time-reversal and



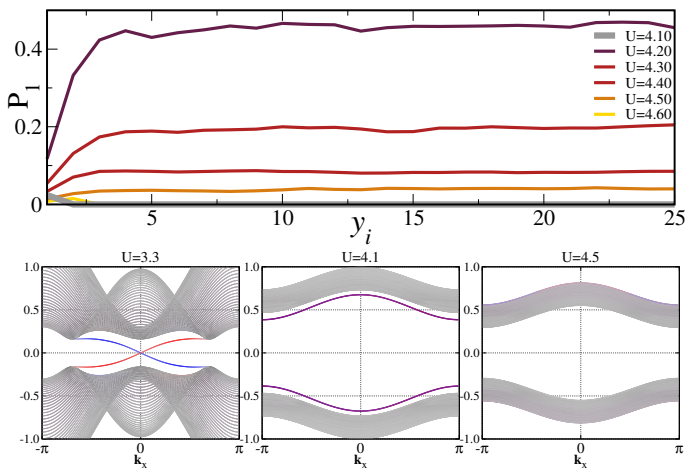


Figure 5. Top panel: Evolution of the low energy band structure of the interacting model at  $M = 1$  and  $J = 0.25U$  on a slab geometry across the QSHI to EI transition. Bottom panels: Evolution of the low energy band structure at  $M = 1$  for  $U = 3.3, 4.1, 4.5$ .

spin  $U(1)$ . The transition between  $P_1$  and  $P_0$  is expected to be first order.

### III. MAGNETO-ELECTRIC NATURE OF THE EXCITONIC INSULATOR

In the EI phase with  $P_1$  order parameter, the breakdown of the symmetries protecting the non-trivial topology of the QSHI, i.e., time-reversal  $\mathcal{T}$ , inversion  $\mathcal{P}$  and spin  $U(1)$  (yet not the product  $\mathcal{PT}$ ), dramatically changes the response to an electromagnetic field. Specifically, the triplet in-plane spin polarization nature of the excitonic order parameter forbids a direct coupling to the electric field and, independently, to the magnetic field. However, the lack of both  $\mathcal{T}$  and  $\mathcal{P}$  symmetries allows the system to couple to the product of magnetic and electric field, i.e. a linear magneto-electric (ME) response [52]. Here, we show that the EI admits a finite ME susceptibility and thus corresponds to a ME insulator. Notably, this state should not be expected to be multi-ferroic because of the absence of magnetic and electric order [52].

In order to study the ME properties, we evaluate the electric dipole response to a magnetic perturbation. Using Green-Kubo formalism and neglecting vertex corrections, we obtain the following expression:

$$\Theta_{\mathbf{q}}^{ab}(\nu_m) = \sum_{\mathbf{k}, n} \frac{\text{Tr} [G(\mathbf{k}, i\omega_n) p^a(\mathbf{k}) G(\mathbf{k} + \mathbf{q}, i\omega_n + i\nu_m) M^b]}{\beta \nu_m} \quad (7)$$

where  $a, b = 1, 2 \equiv x, y$  are the in-plane directions,  $M^a = \frac{1}{2} \Gamma_{a0}$  is the  $a$  component of the spin operator,  $p^a(\mathbf{k})$  is the momentum operator along  $a$ ,  $i\omega_n$  and  $i\nu_m$  are, respectively, fermionic and bosonic Matsubara fre-

quencies and

$$G(\mathbf{k}, i\omega_n) = \left( i\omega_n + \mu - H(\mathbf{k}) - \Sigma(i\omega_n) \right)^{-1},$$

is the interacting Green's function matrix. Given the multi-orbital nature of the Hamiltonian (2) the momentum operator should be evaluated using a generalized Peierls approximation [53–58]. The latter includes additional contributions, stemming from on-site inter-orbital processes that are dipole allowed. Specifically,

$$p_{\alpha\beta}^a(\mathbf{k}) = \partial^a H_{\alpha\beta}(\mathbf{k}) + i\Omega_{\alpha\beta}(\mathbf{k}) d^a$$

where  $\Omega^{\alpha\beta}(\mathbf{k}) = [E_\alpha(\mathbf{k}) - E_\beta(\mathbf{k})]$ ,  $E_\alpha(\mathbf{k})$  are the eigenvalues of the non-interacting Hamiltonian (2), and  $\vec{d} = (\Gamma_{02}, \Gamma_{32})$  is the dipole operator.

In the following we consider the static,  $\nu \rightarrow 0$ , and uniform,  $\mathbf{q} = 0$ , limit of the ME susceptibility. Our results are presented in Fig. 4, where we show the evolution of  $\Theta_{\mathbf{q}=0}^{11}(\nu = 0)$  as a function of  $U$  for finite and zero values of  $J$ . Since the contribution of the group velocity  $\partial_{k_\alpha} H_{\alpha\beta}(\mathbf{k})$  vanishes by symmetry, the ME response is entirely determined by the intra-atomic dipole transitions, which have finite expectation values in the EI phase. Indeed,  $\Theta_{\mathbf{q}=0}^{11}$  is finite only within the EI phase and vanishes otherwise. The magneto-electric susceptibility shows the same dome structure of the order parameter  $P_1$  as a function of  $U$ . The results at  $J = 0$  reported in Fig. 4(b) point out that the ME response vanishes when  $P_0 \neq 0$ , as expected by symmetry. In the EI phase with  $P_1 \neq 0$ , the ME susceptibility is finite and its peak value shifts to lower  $U$  with increasing  $M$ .

At  $J > 0$ , see Fig. 4(a), we observe a substantial change in the magnitude of the ME response. For  $M < 2$ , thus starting from the QSHI, the susceptibility is globally small, while for larger  $M$  the weight of  $\Theta_{\mathbf{q}=0}^{11}$  increases, with seven times larger peak values. Remarkably, for any given  $J$  the largest ME response is reached in proximity of the quantum critical point which, without allowing for  $P_1 \neq 0$ , separates the continuous from the first order topological quantum phase transition [22, 24].

### IV. SLAB GEOMETRY AND EDGE STATES

Finally, we explore the evolution across the QSHI-to-EI phase transition at  $J > 0$  in a slab geometry, i.e. with open boundary conditions along, say, the  $y$  axis, and periodic in the perpendicular direction. In this geometry, the electrons at the boundary experience an effectively larger interaction strength because of the reduced coordination. This effect becomes detectable near the phase transition. In the top panel of Fig. 5, we show the evolution of the  $P_1$  order parameter across the QSHI-EI first order transition with  $M = 1$ . Before the transition, a finite value of the order parameter appears at the boundary, and fast decays in the bulk interior. This is akin a wetting phenomenon that arise since the more correlated

surface favours the nucleation of the EI phase near the first order QSHI-EI transition. This result is remarkable, since it predicts that a QSHI might display a surface layer of excitonic insulator without topological edge states but with finite magnetoelectric response. Increasing  $U$  above the value of the bulk transition, drives the sudden formation of a finite order parameter throughout the sample, as expected for a first order transition. In this case, the order parameter near the boundary is instead reduced with respect to the bulk, consistently with the behaviour of  $P_1$  versus  $U$  for  $M < 2$ , see left panel in Fig. 2.

Further insights can be gained investigating the fate of the helical edge states, see bottom panels of Fig. 5. The plots show the low-energy electronic band structure of the interacting system across the QSHI to EI transition. At small coupling  $U = 3.3$ , well inside the QSHI (left panel), gapless helical edge states well separated from the bulk spectrum are visible. However, at  $U = 4.1$  (middle panel), where the bulk is still a QSHI but an EI wetting layer has formed, see top panel of Fig. 5, edge states still exist but are gapped. On the contrary, for  $U = 4.5$  (right panel), where also the bulk is an EI, the edge states have disappeared inside the bulk continuum.

## V. CONCLUSIONS

In conclusions, we have investigated a canonical model of interacting quantum spin Hall insulators and showed

that for a strong enough electronic correlation the system gets generally unstable towards an excitonic insulator that breaks time-reversal and inversion symmetries, as well as the residual spin  $U(1)$  rotations. This state further evolves into a magnetic Mott insulator upon increasing the interaction strength, where inversion and spin- $U(1)$  symmetry are recovered. We explicitly show that the excitonic insulator has non-zero magneto-electric susceptibility, and thus is a good candidate platform for the realization of correlated multi-ferroic materials. Another remarkable phenomenon that we uncovered is the possible existence of an excitonic insulator wetting layer in a quantum spin Hall insulator.

## VI. ACKNOWLEDGEMENTS

A.A., M.C. and M.F. acknowledge support from H2020 Framework Programme, under ERC Advanced Grant No. 692670 FIRSTORM. A.A. and M.C. also acknowledge support from Italian MIUR through PRIN2017 CEnTral (Protocol Number 20172H2SC4). G.M. was supported by the Swiss FNS/SNF through an Ambizione grant.

- 
- [1] X.-L. Qi and S.-C. Zhang, Topological insulators and superconductors, *Rev. Mod. Phys.* **83**, 1057 (2011).
  - [2] X.-G. Wen, Colloquium: Zoo of quantum-topological phases of matter, *Rev. Mod. Phys.* **89**, 041004 (2017).
  - [3] B. A. Bernevig, T. L. Hughes, and S.-C. Zhang, Quantum Spin Hall Effect and Topological Phase Transition in HgTe Quantum Wells, *Science* **314**, 1757 (2006).
  - [4] M. König, S. Wiedmann, C. Brüne, and *et al.*, Quantum Spin Hall Insulator State in HgTe Quantum Wells, *Science* **318**, 766 (2007).
  - [5] Hsieh D., Qian D., Wray L., Xia Y., Hor Y. S., Cava R. J., and Hasan M. Z., A topological Dirac insulator in a quantum spin Hall phase, *Nature* **452**, 970 (2008), 10.1038/nature06843.
  - [6] D. Hsieh, Y. Xia, L. Wray, D. Qian, A. Pal, J. H. Dil, J. Osterwalder, F. Meier, G. Bihlmayer, C. L. Kane, Y. S. Hor, R. J. Cava, and M. Z. Hasan, Observation of Unconventional Quantum Spin Textures in Topological Insulators, *Science* **323**, 919 (2009).
  - [7] H. Zhang, C.-X. Liu, X.-L. Qi, X. Dai, Z. Fang, and S.-C. Zhang, Topological insulators in Bi<sub>2</sub>Se<sub>3</sub>, Bi<sub>2</sub>Te<sub>3</sub> and Sb<sub>2</sub>Te<sub>3</sub> with a single Dirac cone on the surface, *Nature Physics* **5**, 438 EP (2009).
  - [8] Y. L. Chen, J. G. Analytis, J.-H. Chu, Z. K. Liu, S.-K. Mo, X. L. Qi, H. J. Zhang, D. H. Lu, X. Dai, Z. Fang, S. C. Zhang, I. R. Fisher, Z. Hussain, and Z.-X. Shen, Experimental Realization of a Three-Dimensional Topological Insulator, Bi<sub>2</sub>Te<sub>3</sub>, *Science* **325**, 178 (2009).
  - [9] M. Kargarian and G. A. Fiete, Topological Crystalline Insulators in Transition Metal Oxides., *Phys. Rev. Lett.* **110**, 156403 (2013).
  - [10] I. F. Herbut and L. Janssen, Topological Mott Insulator in Three-Dimensional Systems with Quadratic Band Touching., *Phys. Rev. Lett.* **113**, 106401 (2014).
  - [11] X. Qian, J. Liu, L. Fu, and J. Li, Quantum spin hall effect in two-dimensional transition metal dichalcogenides, *Science* **346**, 1344 (2014).
  - [12] B. Sun, W. Zhao, T. Palomaki, Z. Fei, E. Runburg, P. Malinowski, X. Huang, J. Cenker, Y.-T. Cui, J.-H. Chu, X. Xu, S. S. Ataei, D. Varsano, M. Palummo, E. Molinari, M. Rontani, and D. H. Cobden, Evidence for equilibrium exciton condensation in monolayer wte2, *Nature Physics* **18**, 94 (2022).
  - [13] Y. Jia, P. Wang, C.-L. Chiu, Z. Song, G. Yu, B. Jäck, S. Lei, S. Klemenz, F. A. Cevallos, M. Onyszczak, N. Fishchenko, X. Liu, G. Farahi, F. Xie, Y. Xu, K. Watanabe, T. Taniguchi, B. A. Bernevig, R. J. Cava, L. M. Schoop, A. Yazdani, and S. Wu, Evidence for a monolayer excitonic insulator, *Nature Physics* **18**, 87 (2022).
  - [14] N. Hao and J. Hu, Topological phases in the single-layer fese, *Phys. Rev. X* **4**, 031053 (2014).
  - [15] N. Hao and S.-Q. Shen, Topological superconducting states in monolayer FeSe/SrTiO<sub>3</sub>, *Phys. Rev. B* **92**, 165104 (2015).

- [16] Z. Wang, P. Zhang, G. Xu, L. K. Zeng, H. Miao, X. Xu, T. Qian, H. Weng, P. Richard, A. V. Fedorov, H. Ding, X. Dai, and Z. Fang, Topological nature of the  $\text{FeSe}_{0.5}\text{Te}_{0.5}$  superconductor, *Phys. Rev. B* **92**, 115119 (2015).
- [17] D. Wang, L. Kong, P. Fan, H. Chen, S. Zhu, W. Liu, L. Cao, Y. Sun, S. Du, J. Schneeloch, R. Zhong, G. Gu, L. Fu, H. Ding, and H.-J. Gao, Evidence for majorana bound states in an iron-based superconductor, *Science* **362**, 333 (2018).
- [18] L. Chen, H. Liu, C. Jiang, C. Shi, D. Wang, G. Cui, X. Li, and Q. Zhuang, Topological edge states in high-temperature superconducting  $\text{FeSe}/\text{SrTiO}_3$  films with Te substitution, *Scientific Reports* **9**, 4154 (2019).
- [19] S. Rachel, Interacting topological insulators: a review, *Reports on Progress in Physics* **81**, 116501 (2018).
- [20] Y. Zhang, Y. Ran, and A. Vishwanath, Topological insulators in three dimensions from spontaneous symmetry breaking, *Phys. Rev. B* **79**, 245331 (2009).
- [21] Pesin Dmytro and Balents Leon, Mott physics and band topology in materials with strong spin-orbit interaction, *Nat. Phys.* **6**, 376 (2010).
- [22] A. Amaricci, J. C. Budich, M. Capone, B. Trauzettel, and G. Sangiovanni, First-Order Character and Observable Signatures of Topological Quantum Phase Transitions, *Phys. Rev. Lett.* **114**, 185701 (2015).
- [23] B. Roy, P. Goswami, and J. D. Sau, Continuous and discontinuous topological quantum phase transitions, *Phys. Rev. B* **94**, 041101 (2016).
- [24] A. Amaricci, J. C. Budich, M. Capone, B. Trauzettel, and G. Sangiovanni, Strong correlation effects on topological quantum phase transitions in three dimensions, *Phys. Rev. B* **93**, 235112 (2016).
- [25] L. Crippa, A. Amaricci, N. Wagner, G. Sangiovanni, J. C. Budich, and M. Capone, Nonlocal annihilation of weyl fermions in correlated systems, *Phys. Rev. Research* **2**, 012023 (2020).
- [26] J. C. Budich, B. Trauzettel, and P. Michetti, Time reversal symmetric topological exciton condensate in bilayer hgte quantum wells, *Phys. Rev. Lett.* **112**, 146405 (2014).
- [27] J. Kuneš, Excitonic condensation in systems of strongly correlated electrons, *Journal of Physics: Condensed Matter* **27**, 333201 (2015).
- [28] D. Geffroy, J. Kaufmann, A. Hariki, P. Gunacker, A. Hausoel, and J. Kuneš, Collective modes in excitonic magnets: Dynamical mean-field study, *Phys. Rev. Lett.* **122**, 127601 (2019).
- [29] G. Mazza, M. Rösner, L. Windgätter, S. Latini, H. Hübener, A. J. Millis, A. Rubio, and A. Georges, Nature of symmetry breaking at the excitonic insulator transition:  $\text{ta}_2\text{nise}_5$ , *Phys. Rev. Lett.* **124**, 197601 (2020).
- [30] A. Blason and M. Fabrizio, Exciton topology and condensation in a model quantum spin hall insulator, *Phys. Rev. B* **102**, 035146 (2020).
- [31] L. Windgätter, M. Rösner, G. Mazza, H. Hübener, A. Georges, A. J. Millis, S. Latini, and A. Rubio, Common microscopic origin of the phase transitions in  $\text{ta}_2\text{nise}_5$  and the excitonic insulator candidate  $\text{ta}_2\text{nise}_5$ , *npj Computational Materials* **7**, 210 (2021).
- [32] D. Varsano, M. Palummo, E. Molinari, and M. Rontani, A monolayer transition-metal dichalcogenide as a topological excitonic insulator, *Nature Nanotechnology* **15**, 367 (2020).
- [33] M. Dzero, K. Sun, V. Galitski, and P. Coleman, Topological Kondo Insulators, *Phys. Rev. Lett.* **104**, 106408 (2010).
- [34] M. Dzero, K. Sun, P. Coleman, and V. Galitski, Theory of topological Kondo insulators, *Physical Review B* **85**, 045130 (2012).
- [35] X. Zhang, N. P. Butch, P. Syers, and *et al.*, Hybridization, Inter-Ion Correlation, and Surface States in the Kondo Insulator  $\text{SmB}_6$ , *Phys. Rev. X* **3**, 011011 (2013).
- [36] F. Lu, J. Zhao, H. Weng, Z. Fang, and X. Dai, Correlated Topological Insulators with Mixed Valence, *Phys. Rev. Lett.* **110**, 096401 (2013).
- [37] J. Knolle and N. R. Cooper, Excitons in topological kondo insulators: Theory of thermodynamic and transport anomalies in  $\text{smb}_6$ , *Phys. Rev. Lett.* **118**, 096604 (2017).
- [38] A. Georges, G. Kotliar, W. Krauth, and M. J. Rozenberg, Dynamical mean-field theory of strongly correlated fermion systems and the limit of infinite dimensions, *Rev. Mod. Phys.* **68**, 13 (1996).
- [39] W. Metzner and D. Vollhardt, Correlated Lattice Fermions in  $d = \infty$  Dimensions, *Phys. Rev. Lett.* **62**, 324 (1989).
- [40] E. Müller-Hartmann, Correlated fermions on a lattice in high dimensions, *Zeitschrift für Physik B Condensed Matter* **74**, 507 (1989).
- [41] D. Geffroy, A. Hariki, and J. Kuneš, Excitonic magnet in external field: Complex order parameter and spin currents, *Phys. Rev. B* **97**, 155114 (2018).
- [42] C. A. F. Vaz, J. Hoffman, C. H. Ahn, and R. Ramesh, Magnetoelectric coupling effects in multiferroic complex oxide composite structures, *Advanced Materials* **22**, 2900 (2010).
- [43] F. Thöle, A. Keliri, and N. A. Spaldin, Concepts from the linear magnetoelectric effect that might be useful for antiferromagnetic spintronics, *Journal of Applied Physics* **127**, 213905 (2020).
- [44] A. Amaricci, L. Crippa, A. Scazzola, F. Petocchi, G. Mazza, L. de Medici, and M. Capone, Edipack: A parallel exact diagonalization package for quantum impurity problems, *Computer Physics Communications* **273**, 108261 (2022).
- [45] S. Miyakoshi and Y. Ohta, Antiferromagnetic topological insulator state in the correlated bernevig-hughes-zhang model, *Phys. Rev. B* **87**, 195133 (2013).
- [46] L. Wang, X. Dai, and X. C. Xie, Interaction-induced topological phase transition in the Bernevig-Hughes-Zhang model, *EPL (Europhysics Letters)* **98**, 57001 (2012).
- [47] T. Yoshida, S. Fujimoto, and N. Kawakami, Correlation effects on a topological insulator at finite temperatures, *Phys. Rev. B* **85**, 125113 (2012).
- [48] J. C. Budich, R. Thomale, G. Li, M. Laubach, and S.-C. Zhang, Fluctuation-induced topological quantum phase transitions in quantum spin-Hall and anomalous-Hall insulators, *Phys. Rev. B* **86**, 201407 (2012).
- [49] A. Amaricci, A. Valli, G. Sangiovanni, B. Trauzettel, and M. Capone, Coexistence of metallic edge states and antiferromagnetic ordering in correlated topological insulators, *Phys. Rev. B* **98**, 045133 (2018).
- [50] P. Werner and A. J. Millis, High-Spin to Low-Spin and Orbital Polarization Transitions in Multiorbital Mott Systems, *Phys. Rev. Lett.* **99**, 126405 (2007).



- [51] G. Mazza, A. Amaricci, M. Capone, and M. Fabrizio, Field-driven mott gap collapse and resistive switch in correlated insulators, *Phys. Rev. Lett.* **117**, 176401 (2016).
- [52] W. Eerenstein, N. D. Mathur, and J. F. Scott, Multiferroic and magnetoelectric materials, *Nature* **442**, 759 (2006).
- [53] M. Cruz, M. R. Beltrán, C. Wang, J. Tagüeña Martínez, and Y. G. Rubo, Supercell approach to the optical properties of porous silicon, *Phys. Rev. B* **59**, 15381 (1999).
- [54] T. G. Pedersen, K. Pedersen, and T. Brun Kristensen, Optical matrix elements in tight-binding calculations, *Phys. Rev. B* **63**, 201101 (2001).
- [55] J. M. Tomczak and S. Biermann, Optical properties of correlated materials: Generalized peierls approach and its application to  $\text{VO}_2$ , *Phys. Rev. B* **80**, 085117 (2009).
- [56] P. Wissgott, J. Kuneš, A. Toschi, and K. Held, Dipole matrix element approach versus peierls approximation for optical conductivity, *Phys. Rev. B* **85**, 205133 (2012).
- [57] G. Mazza and A. Georges, Superradiant quantum materials, *Phys. Rev. Lett.* **122**, 017401 (2019).
- [58] J. Li, D. Golez, G. Mazza, A. J. Millis, A. Georges, and M. Eckstein, Electromagnetic coupling in tight-binding models for strongly correlated light and matter, *Phys. Rev. B* **101**, 205140 (2020).